VOL. 5, NO. 8, AUGUST 2010 ISSN 1819-6608
ARPN Journal of Engineering and Applied Sciences


www.arpnjournals.com

RESONANCE FIELDS AND SHIELDING OF A LIVING ROOM EXPOSED TO RADIATIONS FROM A TRANSMITTER BY VECTORIAL FINITE ELEMENT- NEURAL NETWORK METHOD

M. S. H. Al Salameh[1] and R. S. M. Daraghmeh[2]
[1]Department of Electrical Engineering, Jordan University of Science and Technology, Irbid, Jordan
[2]College of Engineering and Technology, Palestine Technical University, Kadoori-Tulkarm, Tulkarm, Palestine
E-Mail: salameh@just.edu.jo

ABSTRACT

This paper presents the application of vectorial finite element-neural network method along with automatic rectangular mesh generation for the prediction of the resonance fields in two dimensional model of a concrete living room. These fields may come from an electromagnetic transmitter such as two-way radio transmitter, amateur radio transmitters, or paging transmitters. The influence of placing a conductive window screen is studied with the aim of reducing the interaction of transmitter stations with humans inside the living room. The electric field is calculated inside the room with various situations: room with door and window, with two windows and furniture, with door and window in addition to furniture, and with a fine metallic window screen. The shielding effectiveness of the window screen is evaluated for different incident angles of the wave. It is found that window screen can provide about 30 dB shielding effectiveness.

Keywords: resonance fields, shielding effectiveness, radiations, transmitter, concrete room, vectorial finite element-neural network method.

1. INTRODUCTION

The demand for wireless communications is rapidly growing. The presence of electromagnetic fields in the environment and its biological effects has also been the topic of recent research. Besides thermal effects, the electromagnetic (EM) fields have the potential to influence the neuron function net and chemical reactions in the cells, especially in period when cell grows and divides [1]. Therefore, it is important to measure the electromagnetic fields (EM) in rooms. A numerical study of the resonance enhancement of the electromagnetic (EM) fields inside living room near the basic antenna stations was presented in [1], where a mathematical approach based on the method of auxiliary sources (MAS) was used to solve for the electromagnetic (EM) fields inside the living room. In the analysis of shielding effectiveness of monolayer and double layer cement shield rooms to HEMP (high electromagnetic protection) [2], the rooms were simulated using finite difference time domain method. The paper [3] discussed indoor wave propagation characteristics of a reinforced concrete building at 1200 MHz band for a portable radio telephone or other indoor radio communication system design. Wave propagation losses through the windows are measured in terms of effective radiation pattern. In [4], the results showed that the concrete thickness and conductivity are the main factors that affect the shielding effectiveness. At low frequencies, the magnetic field shielding effectiveness is not obvious for the pure concrete, but for frequency more than 1 MHz, the wire grid buried in the concrete is effective.

Shielding is one of effective methods which can be used to reduce electromagnetic fields in rooms. Finite element method (FEM) technique can be used in calculating shielding effectiveness. In this paper, we investigate the usability of the vectorial finite element-neural network technique along with automatic mesh generation for evaluating the resonance fields and shielding effectiveness of concrete rooms. The room model used is 2-dimensional. Details of FEM mesh numbering are given. The influence of the shield is studied, and calculated electric field is obtained for a room with various situations such as: room with door and window, with two windows and furniture, with door and window in addition to furniture, and with a fine metallic window screen. The electric field distribution in the shielded (with window screen) room is calculated. Using the shielding in the rooms clearly shows improvement in reducing penetrated EM field values.

2. VECTOR FINITE ELEMENT- NEURAL NETWORK FORMULATION

Finite element method is one of the most powerful and efficient numerical algorithms used to solve general partial differential equations [5, 6]. This is due to the fact that it can handle arbitrary boundaries with extremely irregular shapes and the domain of the problem can include media with varying material characteristics. The basic steps of the finite element method are: domain discretization, formulation of the system of equations, and solution of the system equations. The size of each element in the mesh restricts the maximum frequency which the mesh can accept. If the longest side of the triangular element is Δ, then:

$$\frac{\Delta}{\lambda} \le 0.1,\ \lambda = \frac{\lambda_0}{\sqrt{\varepsilon_r\ \mu_r}} \qquad (1)$$

Where, λ is wavelength (in meters), λ_0 is wavelength in free space, and ε_r, μ_r are relative permittivity and permeability, respectively.

The electromagnetic fields within the problem domain satisfy the vector wave equation:

$$\nabla \times \frac{\nabla \times \vec{E}}{\mu_r} = k_0^{\,2} \varepsilon_c \vec{E},\ \varepsilon_c = \varepsilon_r - j\,\frac{\sigma}{\omega \varepsilon_0} \tag{2}$$

In which, $\vec{E}$ is the electric field vector, k_o the free space wave number, ω radian frequency, ε_0 free space permittivity, and σ electric conductivity in S/m. Since the natural systems seek the state of minimum energy, the fields are equivalently the solution of the variational equation:

$$\delta F(E^*) = 0 \tag{3}$$

Where, $*$ denotes the complex conjugate, and E^* is chosen as the variation parameter in order that the final system of equations will be in terms of the physical quantity *E*. Vector Finite Element method (VFEM) functional for unbounded problems can be represented as [7]:

$$F = \int_{\Omega} \left\{ \frac{\left(\nabla \times \vec{E}\right) \cdot \left(\nabla \times \vec{E}^*\right)}{\mu_r} - k_0^{\,2} \varepsilon_c \vec{E} \cdot \vec{E}^* \right\} d\Omega + j\,\omega \mu_0 \int_s \left(\vec{E}^* \times \vec{H}\right) \cdot \hat{n}\, ds \tag{4}$$

where $\vec{E}$, $\vec{H}$ are electric and magnetic field vectors, respectively, Ω is the solution region, μ_0 is free space permeability, $\hat{n}$ is unit outward normal vector to contour *S* enclosing the solution region Ω, $j = \sqrt{-1}$. When solving open region problems using the finite element method (FEM), the infinite region exterior to the scatterer must be truncated by an artificial outer boundary in order to permit practical implementation on a digital computer. In this paper, the surface S is chosen to conform to the rectangular room as shown in Figure-1.

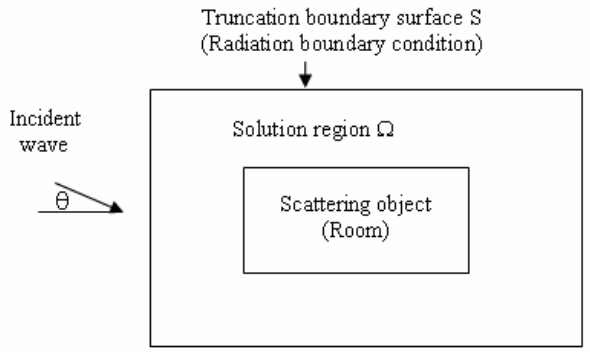

Figure-1. Problem geometry and solution region.

On the other hand, the total energy of the Hopfield Neural Network (HNN) is given by [7]:

$$P = -\frac{1}{2} \sum \sum w_{ij}\, S_i S_j + \sum S_i T_i \tag{5}$$

Where w_{ij} are the neural weights represented by the element matrices of the edge element method, S_i, S_j are the neurons' states represented by the tangential components of the electric field vector in the mesh, and T_i is the neural threshold represented by the incident wave on the room.
It is easy to recognize the similarities between equations (4) and (5). In other words, the solution obtained by minimizing the functional in VFEM is equivalent to the solution obtained from the HNN by minimizing the network's energy.

The radiation boundary condition for transverse electric illumination is [7]:

$$H^s \cdot \hat{z} = \frac{\vec{E}^S \cdot \hat{\phi}}{Z_1},\ Z_1 = \frac{2j\eta_1 k_1 \rho}{2jk_1\rho - 1},\ \eta_1 = \sqrt{\frac{\mu_1}{\varepsilon_1}},$$
$$k_1 = \omega\sqrt{\mu_1 \varepsilon_1} \tag{6}$$

Superscript *s* refers to scattered field, ρ, ϕ, Z are cylindrical coordinates, $\hat{}$ indicates unit vector, and subscript 1 refers to unbounded medium.

In order to solve (4) and (5) numerically, the problem domain must be descritized into finite elements. A typical triangular finite edge element is shown in Figure-2. The edges are denoted by the numbers 1, 2 and 3. Also, the tangential components of the electric field vector evaluated at the centers of the edges are denoted by E_{t1}, E_{t2} and E_{t3}.

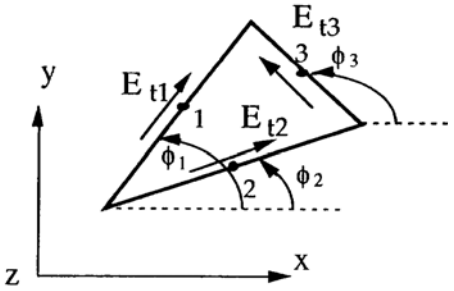

Figure-2. Triangular edge element; edge variables represent neurons' states.

From simple geometrical considerations, each tangential component can be expressed as:

$$E_{ti} = E_{xi} \cos\varphi_i + E_{yi} \sin\varphi_i,\ 0 \le \varphi_i < \pi \tag{7}$$

Where E_{xi} and E_{yi} are the *x* and *y* components of the electric field evaluated at the center of edge *i* (*i*= 1, 2 or 3), and ϕ_i is the azimuthal angle of edge *i* measured from positive *x*-axis. Further, the *x* and *y* components, within each element, are expressed by a linear interpolating function (other higher order interpolating functions can also be used) of *y* and *x*, respectively:

$$E_x = a + cy\,,\; E_y = b + cx \tag{8}$$

Where a, b and c are constants. Combining equations (4)-(8) and using the edge elements discretization, yield the following linear system of equations:

$$[A][E_t] = [B] \tag{9}$$

In which, $[A]$ is a square matrix that involves the shape functions of the triangular edge elements representing the neural network weights, $[E_t]$ is global vector containing the edge variables (the tangential components of the field along the triangles edges) representing the neurons' states, and $[B]$ is the excitation vector representing the thresholds of the neural network. The system of equations (8) can be solved for the electric field vector $[E_t]$.

3. FEM MESH AND SOLUTION ALGORITHM

Finite element models require a definition of the physical area by creating elements that form a finite element mesh. Creating the mesh is one of the most tedious parts of working with finite element models. For this reason, automatic mesh generation methods have been employed to create large groups of elements inside defined polygonal boundaries. One application of the finite element method is the analysis of shielding effectiveness of rooms with the aim of reducing interaction of transmitter stations with humans.

The total number of equations being solved depends on the number of elements in the mesh. As element size decreases, the total number of elements increases. Smaller elements give more accurate results because the differential equations are solved at more points, yielding a better distribution of solution values. However, the increased number of computations also increases the time required to produce a solution. There are tradeoffs between solution accuracy and computation speed. In this paper, the rectangular mesh is divided into layers of triangular elements. The layout of the first layer (3 elements, 5 nodes, 7 edges) is shown in Figure-3, and two layers (12 elements, 12 nodes, 23 edges) are shown in Figure-4. Note that elements numbers are enclosed in small rectangles, edges numbers are written near the arrows, and the remaining are the nodes numbers. The numbering is performed in a counterclockwise manner.

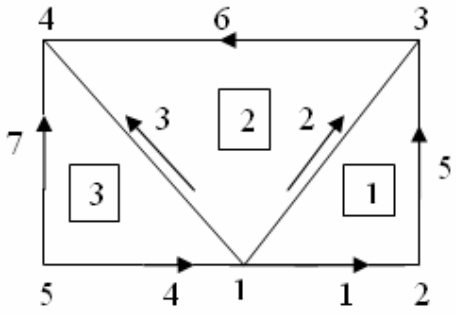

Figure-3. Numbering of nodes, edges and elements in the first layer in the mesh**.**

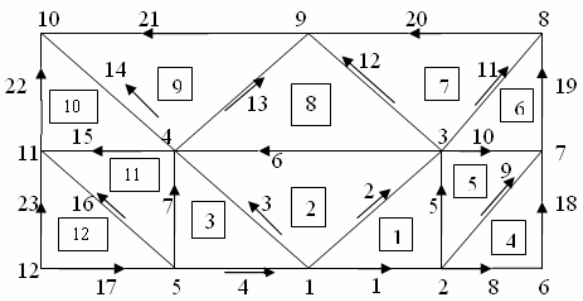

Figure-4. Numbering of two layers in a mesh.

MATLAB was used to write the computer codes. Mesh data can be saved or loaded from ASCII disk file, and this is a convenient way to create an initial mesh. The saved file includes: number of layers, total number of elements, and nodes and edges numberings. The following is a simple saved file which holds the basic information for initialization of rectangular mesh for the first layer shown in Figure-3.

Element number	node numbering	edges numbering
1	1 2 3	1 5 2
2	1 3 4	2 6 3
3	1 4 5	3 7 4

Programs for mesh refinement were also written. After that we used the following procedure (shown in Figure-5) to solve the problem:

a) Descritize the domain of the rectangular FEM mesh.
b) Predetermine convergence criterion (threshold error ε_s) (chosen to be 10^{-4}).
c) Specify material parameters $(\varepsilon_r, \mu_r, \sigma)$ for all elements.
d) Define the radiation boundary condition.
e) Generate the vector finite element mesh.
f) Start iterations to compute the electric field at the edges of each element according to the Finite Element–Neural Network method [7].
g) When the error is below the threshold error value in step 1, stop and give results. The error is defined as the difference between the two sides of equation (9). Note that when electric field iteration values are substituted for $[E_t]$ in equation (9), the equality will not hold unless we reach the exact solution for $[E_t]$.

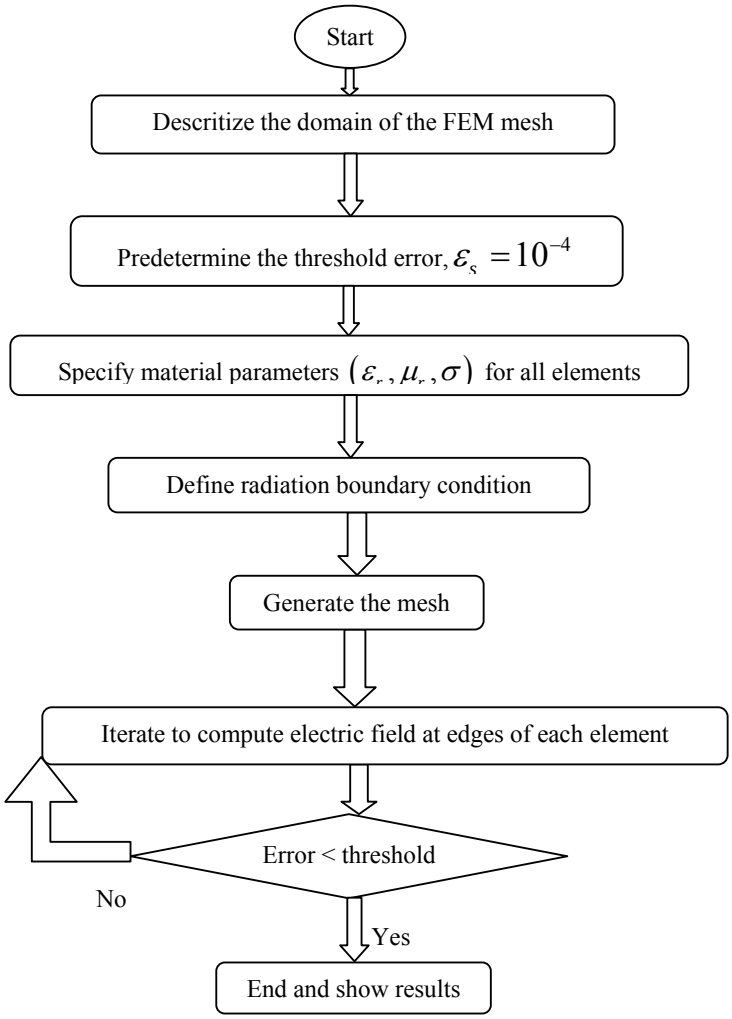

Figure-5. Flowchart that describes the solution algorithm.

RESULTS

Some examples are solved to show the applicability of the finite edge element- neural network method. Towards that end, a room with different configurations is considered: A. room with door and window, B. room with two windows and furniture, C. room with window and door and furniture, and D. Room with shielded window. MATLAB codes were written to solve these problems. However, before proceeding with the room solutions, and in order to validate the written computer programs, a metallic shielding enclosure was solved and the results compared very well with the solutions presented in [8].

A. Room with door and window

The cross-section of the room (6m×3m) is shown in Figure-6. A wave from a transmitter impinges on the room. The room is in the far zone of the transmitter and

thus the wave is assumed plane wave. The room is considered to be made of concrete. The concrete parameters chosen are: relative permittivity $\varepsilon_r = 10 - j\,2.8$, conductivity $\sigma = 0.00389$ S/m, relative permeability $\mu_r = 10$ [9]. The transmitting frequency of 25 MHz is chosen to correspond to the first resonance of the room, i.e., when the room length is half wavelength. In order to calculate the electromagnetic fields in the room, the mesh is divided into 1452 triangular elements with number of edges = 2233. In this case, the size of the truncating boundary (24m×22m) was adjusted until stable results were obtained. The field distribution is shown in Figure-7 for zero incidence angle. Due to resonance, the field inside the room is higher than outside. The resonance pattern is readily observed in the room where the field is largest in the middle of the room and decreases steadily towards the ends of the room. In addition, note that the field magnitude is highest along the window opening, since the lossy and conductive walls of the room block the incident wave. For other incidence angles, the results are summarized in Figure-8. In this problem high resonance fields arise especially at grazing incidence. It is noticed from Figure-8 that the electric field decreases with increasing the incidence angle. The maximum resonance field at θ = 0° was (1.6 V/m) and only 0.357 V/m at θ = 85°.

B. Room with furniture and two windows

The room geometry is illustrated in Figure-9. The furniture was arbitrarily chosen to have the following parameters: $\mu_r = 1, \varepsilon_r = 3 - j\,2$, $\sigma = 0.0027$ s/m; the algorithm is valid for any values of material parameters. The piece of furniture dimensions were chosen as: width of 1.2 m and height of 0.6 m. The frequency of the incident wave is 25 MHz. We see from the electric field distribution shown in Figure-10 that high field values appear in the middle of the room when the angle of the incident wave is zero. However, the field is lower than that of the room without the piece of furniture. It seems that the furniture has the effect of shifting the resonance frequency. So, we expect that the field would be higher at a lower resonant frequency as will be seen in the examples below. Again the field values decrease with increasing the angle of the incident wave (Figure-11). Note that the rate of decrease of the field is perturbed around the 45° incidence angle. This may be explained as follows: it is evident from Figure-9 that at 45° incidence, the incident wave directly strikes the furniture inside the room causing additional reflection of the wave which may locally enhance the field strength. The truncation boundary was 24m×24m, number of elements = 1728, edges = 2652.

C. Room with furniture, opened door and window

The room geometry is shown in Figure-12. The piece of furniture has the same size and material parameters as that described in the previous example. Figures 13 and 14 reveal that the high field values occur in the middle of the room when the angle of incidence is zero. The FEM mesh has number of elements= 1728 and edges = 2652. The maximum resonance field at θ = 0° was (1.1 V/m) and only 0.22 V/m at θ = 85°. As in the other examples, the maximum field at resonance decreases with increasing the angle of incidence as shown in Figure-14. In Figure-15, we display the relation between the electric field and frequency where it is evident that the field is a strong function of frequency. Figure-15 shows that although the field at 25 MHz is lowered in the presence of the furniture, it is significantly higher at lower and higher frequencies. In other words, the furniture has the effect of shifting the resonance frequency of an empty room.

D. Shielded window with a fine metallic screen

Consider the room with the window shielded by a fine metallic screen as shown in Figure-16. Since the metallic screen is very fine (i.e., distance between adjacent filaments of the screen is much smaller than the wavelength), it can be represented by a continuous metallic sheet. From Figure-17, the maximum electric field at θ=0° is only 0.12 V/m, whereas the maximum field for this room with unshielded window is 7.6 V/m (the field distribution for the case of a room with only a window is not shown in order to limit the number of pages of the paper). The shielding effectiveness (SE) of this screen is defined as [10], [11]:

$$SE = 20\ log\ \frac{E_O}{E_1}, \qquad \text{in dB}$$

Where E_0 is the maximum electric field at resonance without shielding, and E_1 is the maximum electric field at resonance with shielding. Table-1 shows that the window metallic screen is a viable tool to inhibit field penetration. SE for the window screen is about 30 dB for different incidence angles of the wave. Note that in all the presented examples, the field mainly enters the room from the window (on the side of the incident wave). On the contrary, the field mainly enters from the room walls in the case of screened window as can be seen in Figure-17. The penetrating field decreases almost linearly with the incidence angle as shown in Figure-18.

Table-1. Shielding effectiveness of the room with shielded window.

Max field without shielding in V/m	Max field with shielding in V/m	Shielding effectiveness in dB	Incidence angle in degrees
7.6	0.12	36	0
3.4	0.09	31.5	15
1.58	0.06	28.4	30
1.3	0.04	30.2	45
1.14	0. 034	30.5	60
0.84	0.03	28.9	85

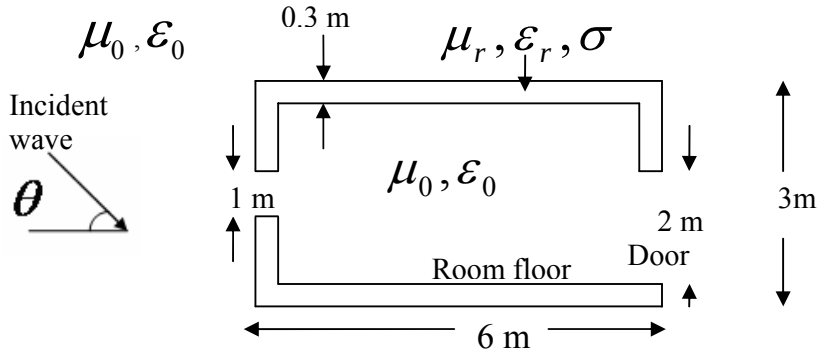

Figure-6. Wave incident on a room with door and window.

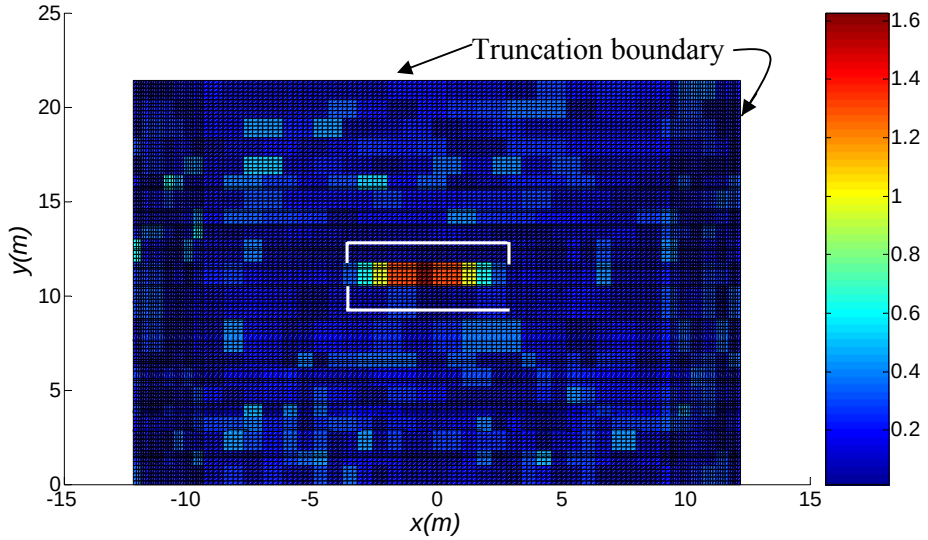

Figure-7. Electric field amplitude at resonance inside and near a room (6m×3m) with door and window. The color bar indicates electric field amplitude in V/m. Incidence angle θ = 0°. White lines are room boundaries.

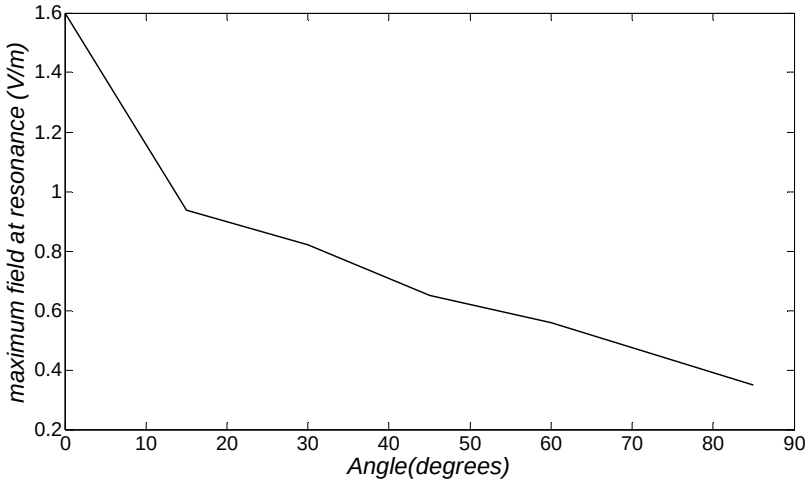

Figure-8. Maximum field in room (with door and window) at resonance vs. incidence angle.

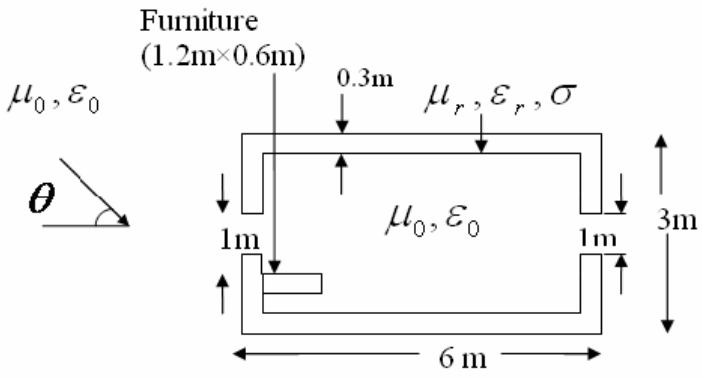

Figure-9. The room with furniture and two windows.

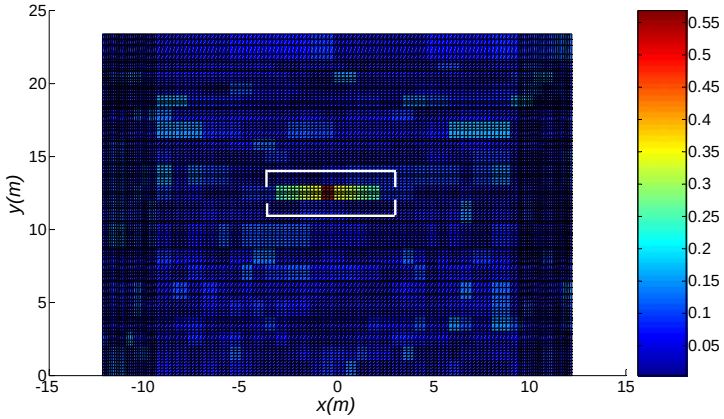

Figure-10. Electric field amplitude at resonance inside and near the room with furniture and two windows ($\theta = 0°$).

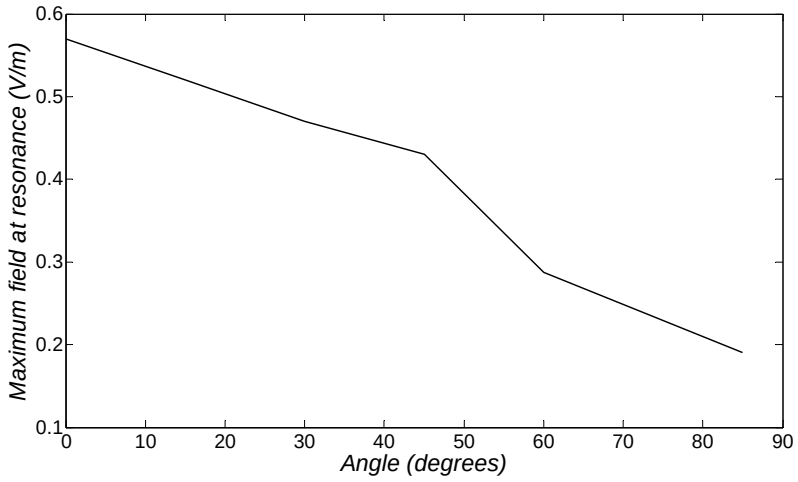

Figure-11. Maximum field in room (with furniture and two windows) at resonance vs. incidence angle.

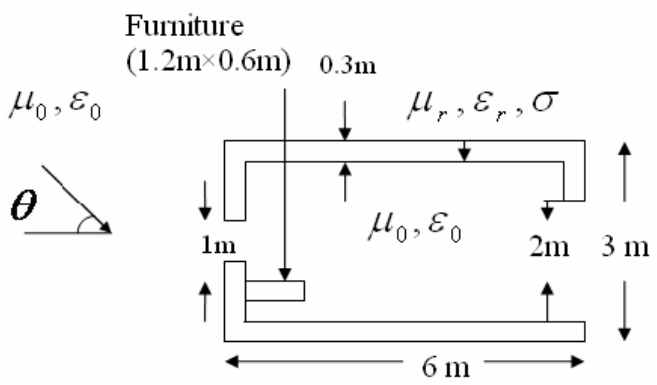

Figure-12. The room with furniture, opened door and window.

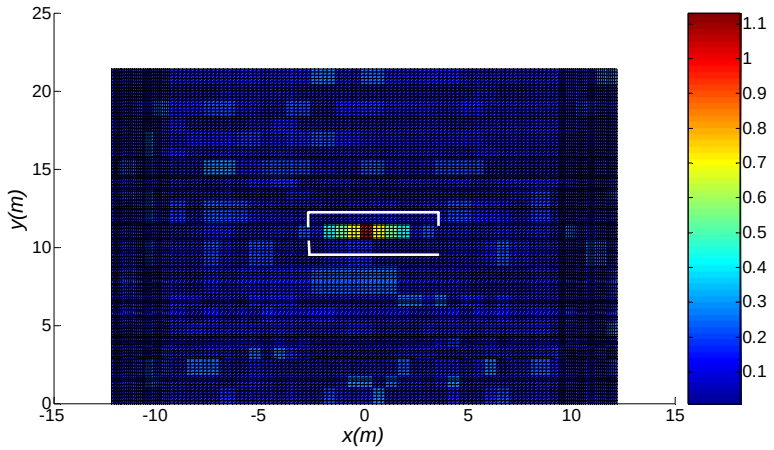

Figure-13. Electric field amplitude at resonance inside and near the room with furniture, opened door and window ($\theta = 0°$).

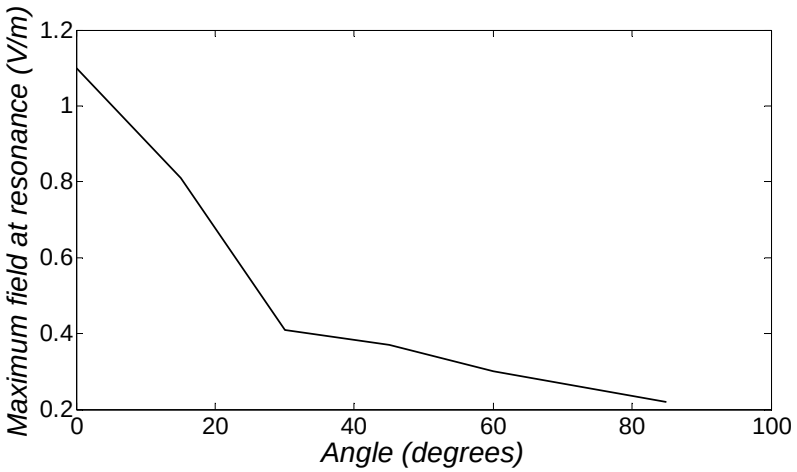

Figure-14. Maximum field in room (with opened door, furniture and window) at resonance vs. incidence angle.

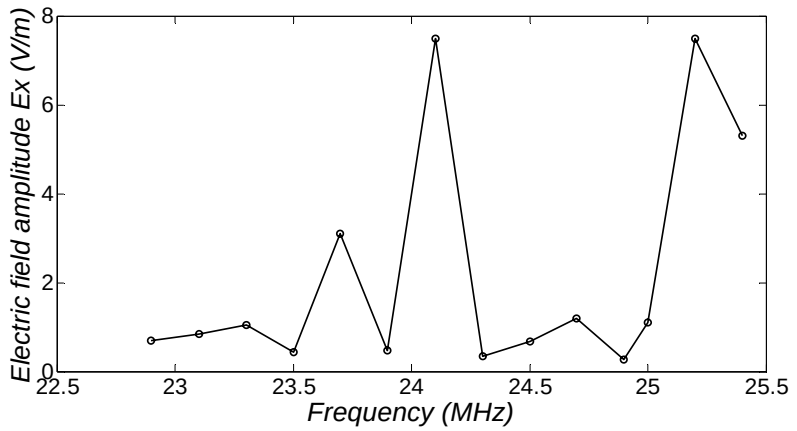

Figure-15. Effect of changing frequency: Maximum electric field amplitude inside the room (with opened door, furniture and window) as a function of frequency, at $\theta = 0°$.

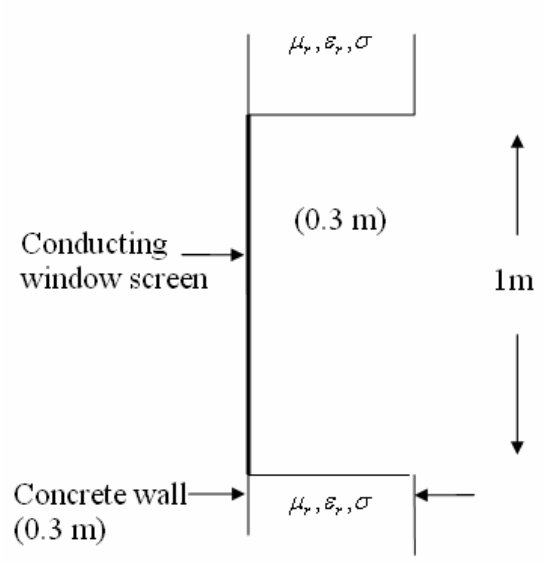

Figure-16. The window is shielded by a fine metal screen.

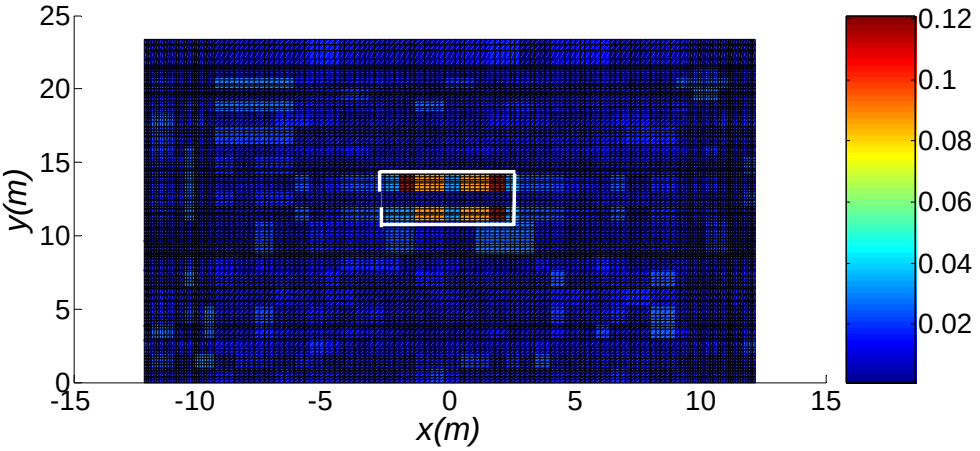

Figure-17. Electric field amplitude at resonance inside and near the room with window metallic screen, θ = 0°.

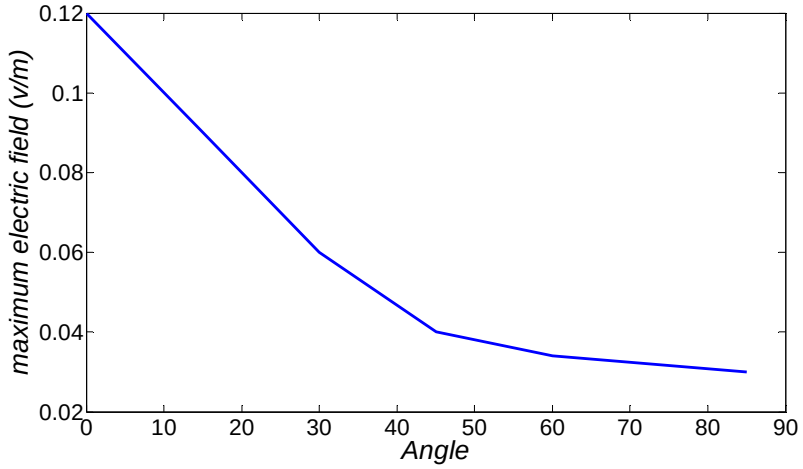

Figure-18. Maximum field in the room with screened window at resonance as a function of incidence angle.

CONCLUSIONS

The finite element neural network method can be used to understand the field behavior inside the room for a number of parameters like frequency, angle of incidence, and location inside the room. The field was solved for different room configurations: room with door and window, with two windows and furniture, with door and window in addition to furniture, and with a fine metallic window screen. The shielding effectiveness (SE) of the window screen was about 30 dB for different angles of the incident wave. Thus, the fine metallic window screen is efficient in reducing the field penetration into the room. It was observed that the electric field inside the room decreases as the incident angle of the incident plane wave increases. The presence of objects inside the room such as the furniture affects the field distribution in the room. As expected, the maximum field at resonance inside the room is larger than the incident field due to multiple reflections from the inner surfaces in the room. The various exposure guidelines such as the ICNIRP (International Commission on Non-Ionizing Radiation Protection) reference levels of human exposure to electric and magnetic fields are usually based on the field values in the region outside the rooms. The results here show that these limits are not adequate as the field inside the room may become larger than outside the room at resonance.

REFERENCES

[1] D. K. akulia, K. Tavzarashvili, V. Tabatadze and R. Zaridze. 2003. Investigation of the field distribution inside rooms located near the basic antenna stations. Proceedings of 8th international seminar on direct and inverse problems of electromagnetic and acoustic wave theory. Lviv, Ukraine. pp. 162-165.

[2] Gue Fei and Zhou Bihua. 2008. Analysis of shielding effectiveness of monolayer and double layer cement shield rooms to HEMP. China-Japan joint Microwave Conference, Shanghai. pp. 505-508.

[3] J. Horikishi, K. Tanaka and T. Morinaga. 1986. 1.2 GHz Band Wave Propagation Measurements in Concrete Building for Indoor Radio Communications. IEEE Transactions on Magnetics. 35(4): 146-152.

[4] Zhibin Zhao, Xiang Cui, Lin li. 2008. Analysis of Shielding Performance of Reinforced Concrete Structures Using the Method of Moments. IEEE Transactions on Magnetics. 44(6): 1474-1477.

[5] Saeed Moaveni. 2007. Finite Element Analysis: Theory and Application with Ansys. 3rd Edition. Mankato, Prentice Hall.

[6] J. Jin. 2002. The Finite Element Method in Electromagnetic. John Wiley and Sons, Inc., New York.

[7] M. S. Al Salameh and E. T. Al Zuraiqi. 2008. Solutions to Electromagnetic Compatibility Problems using Artificial Neural Networks Representation of Vector Finite Element Method. IET Microwaves, Antennas and Propagation. 4: 348-357.

[8] M. S. Tharf Al Salameh and G. I. Costache. 1993. Edge Element- Scattering Amplitude Solution to Electromagnetic Leakage into Shielding Enclosures. IEEE Conference on EMC. Dallas, TX, USA. pp. 9-13, 202-206.

[9] R. A. Dalk, C. L. Holloway. 2000. Effects of Reinforced Concrete Structures on RF communications. IEEE Trans. EMC. 4(4): 486-496.

[10] H. W. Ott. 1988. Noise Reduction Techniques in Electronic Systems. 2nd Ed. Wiley-Interscience, New York.

[11] Ooi Tian Hock and Foo Chew Houw. 1999. Automated Shielding Effectiveness Test System for Shielded Enclosures. 1999 International Symposium on Electromagnetic Compatibility, Tokyo, Japan. pp. 682-685.